ISSN 1070-3284, Russian Journal of Coordination Chemistry, 2022, Vol. 48, No. 6, pp. 371–378. © Pleiades Publishing, Ltd., 2022.
Russian Text © The Author(s), 2022, published in Koordinatsionnaya Khimiya, 2022, Vol. 48, No. 6, pp. 370–377.

Platinum(II) Complexes $[Ph_3PCH_2OH]_2[PtCl_4]$ and *trans*-$PtCl_2(PPh_3)_2]\cdot CHCl_3$: Synthesis, Crystal Structures, and Thermal Stability

A. R. Zykova[a], *, V. V. Sharutin[a], O. K. Sharutina[a], and O. S. El'tsov[b]

[a] *South Ural State University (National Research University), Chelyabinsk, Russia*
[b] *Ural Federal University, Chemical Technological Institute, Yekaterinburg, Russia*
**e-mail: zykovaar@susu.ru*

Received October 11, 2021; revised October 20, 2021; accepted October 22, 2021

Abstract—The divalent platinum complexes $[Ph_3PCH_2OH]_2[PtCl_4]$ (**I**) and *trans*-$[PtCl_2(PPh_3)_2]$ (**II**·$CHCl_3$) are synthesized by the reaction of hexachloroplatinic(IV) acid with (hydroxymethyl)triphenylphosphonium chloride in an acetonitrile–water (4 : 1) mixture. The dissolution of crystals of complex **I** in diethyl sulfoxide affords crystals of complex **II**. The structures of the complexes are determined by IR and NMR spectroscopy and X-ray diffraction (CIF files CCDC nos. 2055552 (**I**) and 2055809 (**II**·$CHCl_3$)). The platinum atoms in complexes **I** and **II**·$CHCl_3$ have a planar square coordination. The crystal structures of complexes **I** and **II**·$CHCl_3$ are stabilized by interionic and intermolecular contacts. The thermal analysis of the crystals of complex **I** shows its instability and mass loss at 170 and 305°C. The thermogravimetric curve of the crystals of complex **II**·$CHCl_3$ shows a mass loss of the solvent molecule at 170°C and a smooth descend of the thermogravimetric curve after the platform reaches 310°C.

Keywords: (hydroxymethyl)triphenylphosphonium tetrachloroplatinate, dichlorobis(triphenylphosphine)-platinum, X-ray diffraction, thermal stability

DOI: 10.1134/S1070328422060082

INTRODUCTION

Coordination platinum complexes are of fundamental interest due to a broad range of applicability. Since the discovery of the cytotoxic effect, the platinum complexes have actively been used in chemotherapy [1–6]. In addition, they exhibit anti-inflammatory, antimicrobial, and antifungal activities [7, 8] and catalytic properties [9–12]. The platinum complexes bearing amines, sulfides, phosphine, and stibines as ligands are widely studied in various areas of organometallic chemistry [13, 14]. Lipophilic cations $[Ph_3PR]^+$ are important precursors for the platinum complexes containing organic ligands [15]. The tetraorganylphosphonium salts manifest disinfectant properties [16–19].

A few platinum complexes with mononuclear tetrachloroplatinate anions and organyltriphenylphosphonium cations were described [20–24]. The most efficient method for the synthesis of these compounds is presented by the reactions of tetraorganylphosphonium halides with tetrachloroplatinic acid potassium salt in water [21].

We have previously studied the reactions of complex acid H_2PtCl_6 with organyltriphenylphosphonium chlorides in acetonitrile affording the corresponding hexachloroplatinates(IV) [25]. In the present work we show that this reaction with (hydroxymethyl)triphenylphosphonium chloride in an acetonitrile–water (4 : 1) mixture is not typical but affords a mixture of new platinum(II) complexes: $[Ph_3PCH_2OH]_2[PtCl_4]$ (**I**) and *trans*-$[PtCl_2(PPh_3)_2]$ (**II**·$CHCl_3$). We synthesized the new complexes and studied their structures and thermal stability.

EXPERIMENTAL

All procedures associated with the synthesis of new complexes were carried out in air using acetonitrile and distilled water. Hexachloroplatinic acid was synthesized using a described procedure [26].

The IR spectra of the complexes were recorded on a SHIMADZU IRAffinity-1S FT-IR spectrometer in a range of 4000–400 cm^{-1}. Solid samples were prepared in KBr pellets.

^1H and ^{31}P NMR spectra were detected on a Bruker AVANCE NEO NMR spectrometer (600 MHz). Chemical shifts were measured relative to TMS as the internal standard for ^1H and relative to H_3PO_4 as the external standard for ^{31}P. Elemental analysis was car-

ried out on a Carlo Erba CHNS-O EA1108 CHNS-O elemental analyzer.

Thermogravimetry (TG) and differential scanning calorimetry (DSC) were conducted using a STANetzschSTA 449C Jupiter thermal analyzer in air (dynamic conditions, temperature range 0–380 K).

Synthesis of (hydroxymethyl)triphenylphosphonium tetrachloroplatinate(II) (I). A solution of hexachloroplatinic acid hexahydrate (0.5 g, 2.0 mmol) in an acetonitrile–water mixture (5 mL) was poured to a solution of (hydroxymethyl)triphenylphosphonium chloride (0.66 g, 2.0 mmol) in an acetonitrile–water (4 : 1) mixture. The resulting solution was concentrated, and the formation of crystals of two types was observed: red-brown crystals of complex **I** (0.37 g, 40%, T_m = 195°C) and colorless crystals of compound **II**. A mixture of the crystals was separated by recrystallization from chloroform. Since the crystals of complex **I** were not dissolved, they were filtered off and dried.

IR of **I** (ν, cm^{-1}): 3255 (O–H), 3039 (C_{Ar}–H), 1484 (C_{Ar}), 1438 (C_{Ar}). ^{1}H NMR of **I** (DMSO-d_6; 600 MHz; δ, ppm): 4.80 (m, 1H, OH); 4.67 (m, 2H, CH_2); 7.42 (d, 6H, *m*-H_{Ph}, $^2J_{HH}$ = 7.81 Hz); 7.55 (m, 6H, *p*-H_{Ph}); 7.67 (m, 2H, *o*-H_{Ph}). ^{31}P NMR of **I** (δ, ppm): 25.56.

For $C_{38}H_{36}O_2P_2Cl_4Pt$		
Anal. calcd., %	C, 49.40	H, 3.90
Found, %	C, 49.36	H, 3.93

Synthesis of *trans*-dichlorobis(triphenylphosphine)-platinum (II·$CHCl_3$). The crystals of complex **I** (0.1 g) were dissolved in diethyl sulfoxide (3 mL). The solution was concentrated, and the decoloration of the solution and formation of colorless crystals were observed. The yield of complex **II** was 0.045 g (53%), T_m = 308°C. Solvate **II**·$CHCl_3$ was formed by the recrystallization of *trans*-[$(Ph_3P)_2PtCl_2$] from chloroform. The IR spectra and T_m of complexes **II** and **II**·$CHCl_3$ coincided.

IR of **II**·$CHCl_3$ (ν, cm^{-1}): 3052 (C_{Ar}–H), 1480 (C_{Ar}), 1434 (C_{Ar}). ^{1}H NMR of **II**·$CHCl_3$ (DMSO-d_6; 600 MHz; δ, ppm): 7.27 (m, 2H, *o*-H_{Ph}); 7.42 (m, 9H, *m*- + *p*-H_{Ph}), 7.95 (s, H, $CHCl_3$). ^{31}P NMR (δ, ppm): 13.83.

For $C_{37}H_{31}P_2Cl_5Pt$		
Anal. calcd., %	C, 48.81	H, 3.41
Found, %	C, 48.76	H, 3.43

X-ray diffraction (XRD) of the crystals of complexes **I** and **II**·$CHCl_3$ was carried out on a D8 QUEST Bruker automated four-circle diffractometer (MoK_α radiation, λ = 0.71073 Å, graphite monochromator) at 296(2) K. The structures were solved by a direct method, and positions and temperature parameters of non-hydrogen atoms were refined in the isotropic and then anisotropic approximation by full-matrix least squares. Hydrogen atoms were placed in the geometrically calculated positions and included into refinement by the riding model. Data were collected and edited, unit cell parameters were refined, and an absorption correction was applied using the SMART and SAINT-Plus programs [27]. All calculations on structure determination and refinement were performed using the SHELXL/PC [28] and OLEX2 [29] programs. The crystallographic data and main structure refinement parameters are given in Table 1. Selected bond lengths and bond angles are listed in Table 2.

The full tables of atomic coordinates, bond lengths, and bond angles were deposited with the Cambridge Crystallographic Data Centre (CIF files CCDC nos. 2055552 (**I**) and 2055809 (**II**·$CHCl_3$); http://www.ccdc.cam.ac.uk).

RESULTS AND DISCUSSION

The reaction of equimolar amounts of hexachloroplatinic acid hexahydrate with (hydroxymethyl)triphenylphosphonium chloride in an acetonitrile–water mixture is accompanied by the formation of red-brown crystals of (hydroxymethyl)triphenylphosphonium tetrachloroplatinate(II) (**I**) and colorless crystals of *trans*-dichlorobis(triphenylphorphine)platinum (**II**). The latter were isolated as solvate *trans*-[$PtCl_2(PPh_3)_2$] (**II**·$CHCl_3$) after recrystallization from chloroform.

Evidently, the phosphonium cation is transformed during the reaction with the elimination of formaldehyde that reduces Pt(IV) to Pt(II).

$$[Ph_3PCH_2OH]Cl + H_2PtCl_6\cdot 6H_2O \xrightarrow[(2)\ CHCl_3]{(1)\ CH_3CN-H_2O} \underset{\textbf{(I)}}{[Ph_3PCH_2OH]_2[PtCl_4]} + \textit{trans}\text{-}\underset{(\textbf{II}\cdot CHCl_3)}{[PtCl_2(PPh_3)_2]\cdot CHCl_3}.$$

Table 1. Crystallographic data and experimental and structure refinement parameters for compounds **I** and **II**·$CHCl_3$

Parameter	Value	
	I	**II**·$CHCl_3$
FW	923.50	1819.79
T, K	293.15	293.15
Crystal system	Monoclinic	Monoclinic
Space group	$P2_1/n$	$C2/m$
a, Å	9.103(4)	12.392(6)
b, Å	15.709(5)	14.184(7)
c, Å	13.155(4)	11.660(6)
α, deg	90	90
β, deg	105.826(15)	117.550(17)
γ, deg	90	90
V, Å^3	1809.8(11)	1817.1(17)
Z	2	1
ρ_{calc}, g/cm^3	1.695	1.663
μ, mm^{-1}	4.294	4.343
F(000)	912.0	892.0
Range of θ, deg	6.104–56.998	6.596–56.996
Number of measured reflections	41 121	21 027
Number of independent reflections	4571	2400
R_{int}	0.0272	0.1623
Refinement variables	221	144
GOOF	1.092	1.041
R factors for $F^2 > 2\sigma(F^2)$	$R_1 = 0.0178$, $wR_2 = 0.0387$	$R_1 = 0.0323$, $wR_2 = 0.0807$
R factors for all reflections	$R_1 = 0.0244$, $wR_2 = 0.0413$	$R_1 = 0.0323$, $wR_2 = 0.0807$
Residual electron density (min/max), e/Å^3	−0.39/0.81	−1.48/1.29

Formaldehyde and triphenylphosphine are formed under the treatment of (hydroxymethyl)triphenylphosphonium with potassium carbonate [30].

$$Ph_3P^+CH_2OH \xrightarrow{K_2CO_3} [CH_2O] + Ph_3P.$$

The dissolution of the crystals of complex **I** in diethyl sulfoxide (Et_2SO) is accompanied by the gradual decoloration of the solution and formation of colorless crystals of complex **II** rather than the assumed product of solvent molecule insertion into the coordination sphere of platinum.

$$\underset{\textbf{(I)}}{[Ph_3PCH_2OH]_2[PtCl_4]} \xrightarrow{Et_2SO} \underset{\textbf{(II)}}{\textit{trans}\text{-}[PtCl_2(PPh_3)_2]} + 2CH_2O + 2HCl.$$

The transformation of complex **I** into **II** is worth of detailed study. The measurement of the melting point of complex **I** in an open capillary showed the decoloration of the red-brown crystals of the complex at 195–197°C. The complete decomposition of the crystals is observed at 308–310°C. We assumed that complex **I** transformed into complex **II** in this temperature range.

The DSC method in a temperature range of 0–380 K was used for the evaluation of the thermal behavior of the complexes.

The thermal effects are observed on the DCS curve of complex **I** on heating: an intense endothermal signal in a range of 165–225°C and a low-intensity signal transforming into the exothermal one at 290–320°C.

Table 2. Selected bond lengths and bond angles in the structures of compounds **I** and **II**·$CHCl_3$

Bond	*d*, Å	Bond	*d*, Å
		I	
Pt(1)Cl(1)	2.3121(11)	P(1)–C(11)	1.790(2)
Pt(1)Cl(1')	2.3121(11)	P(1)–C(1)	1.794(2)
Pt(1)–Cl(2)	2.3044(10)	P(1)–C(21)	1.796(2)
Pt(1)–Cl(2')	2.3044(10)	P(1)–C(7)	1.822(2)
		II·$CHCl_3$	
Pt(1)–P(1)	2.3224(17)	P(1)–C(11)	1.854(4)
Pt(1)–P(2)	2.3223(17)	P(1)–C(1)	1.796(4)
Pt(1)–Cl(1)	2.3119(18)	P(1)–C(21)	1.828(4)
Pt(1)–Cl(2)	2.3119(18)		
Angle	ω, deg	Angle	ω, deg
		I	
Cl(1')Pt(1)Cl(1)	180.0	C(11)P(1)C(1)	109.28(10)
Cl(2)Pt(1)Cl(1')	90.43(3)	C(11)P(1)C(21)	110.02(10)
Cl(2')Pt(1)Cl(1')	89.57(3)	C(11)P(1)C(7)	107.95(12)
Cl(2')Pt(1)Cl(1)	90.43(3)	C(1)P(1)C(21)	110.90(10)
Cl(2)Pt(1)Cl(1)	89.57(3)	C(1)P(1)C(7)	109.81(11)
Cl(2)Pt(1)Cl(2')	180.0	C(21)P(1)C(7)	108.84(11)
		II·$CHCl_3$	
P(2) Pt(1)P(1)	180.0	Cl(1)Pt(1)Cl(2)	180.0
Cl(1)Pt(1)P(2)	87.48(5)	C(11)P(1) Pt(1)	109.48(15)
Cl(2)Pt(1)P(1)	87.47(5)	C(21)P(1) Pt(1)	113.41(17)
Cl(1)Pt(1)P(1)	92.52(5)	C(1)P(1)C(1)	119.6(2)
Cl(2)Pt(1)P(2)	92.53(5)	C(1)P(1)Pt(1)	118.95(16)

The DSC curve of complex **II**·$CHCl_3$ exhibits the exothermal signal at 295–340°C. The TG curve of complex **I** exhibits a mass loss of 13.91% at 165–215°C corresponding to the release of $2CH_2O$ and HCl (theor. 13.51%). According to the calorimetry data, the transformation starts at 171°C (Fig. 1). The substance melts at 305°C (melting point of *trans*-$[PtCl_2(PPh_3)_2]$ is 310°C [31]). The TG curve of **II**·$CHCl_3$ shows a mass loss of 15.51% in a temperature range of 300–360°C related to the release of the solvate molecule of the solvent, and the TG curve descends smoothly after 310°C. The obtained DSC and TG data confirm the instability of complex **I** and its transformation into **II**·$CHCl_3$ upon the thermal treatment.

The structures of the synthesized complexes were proved by IR spectroscopy, ^1H and ^{31}P NMR spectroscopy, elemental analysis, and XRD.

The IR spectra and T_m of colorless crystals of complexes **II** and **II**·$CHCl_3$ synthesized via Schemes 3 and 1, respectively, are identical. The IR spectra of compounds **I** and **II**·$CHCl_3$ contain characteristic bands of stretching vibrations of the carbon skeleton of the aromatic fragments: 1484, 1438 cm^{-1} for complex **I** and 1480, 1434 cm^{-1} for **II**·$CHCl_3$. Medium-intensity bands at 3039 (**I**) and 3052 cm^{-1} (**II**·$CHCl_3$) corresponding to the C_{Ar}–H stretching vibrations are also observed. The spectrum of complex **I** exhibits a broadened band at 3255 cm^{-1} caused by the ν(O–H) stretching vibrations of the O–H bond.

The ^1H NMR spectra exhibit signals of the proton of the phenyl rings in a downfield range of 7.36–7.67 ppm. The multiplet signal of the proton of the –OH hydroxyl group in complex **I** is detected at 4.80 ppm. The spectrum of **II**·$CHCl_3$ contains the signal of the solvate $CHCl_3$ molecule as a singlet at 7.95 ppm. The ^{31}P NMR spectra exhibit single signals of phosphorus at 25.56 (**I**) and 13.83 ppm (**II**·$CHCl_3$).

According to the XRD data, the $[Ph_3PCH_2OH]^+$ cation of complex **I** has a tetrahedral coordination of the phosphorus atom with the aryl ligands and hydroxymethyl substituent at the vertices of the tetrahedron (Fig. 2a). The hydroxymethyl group is disor-

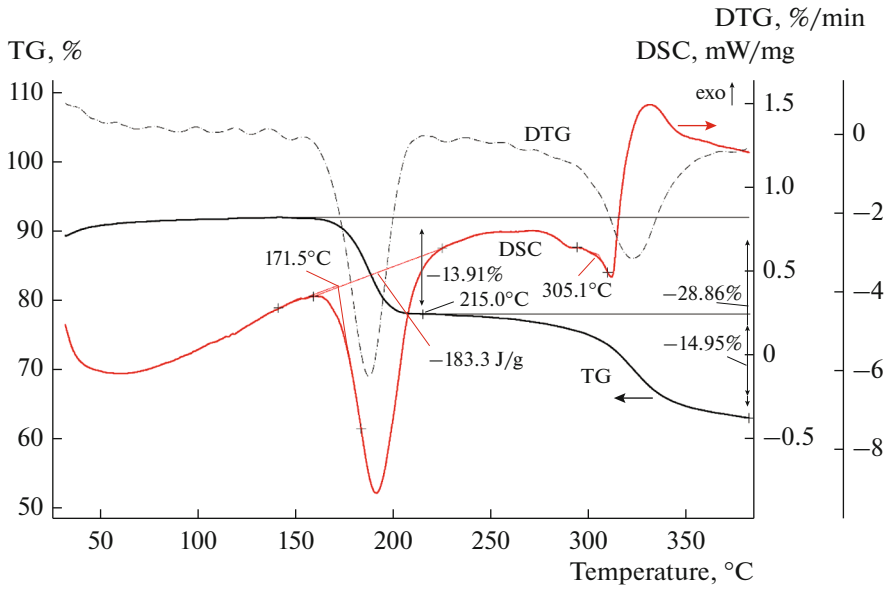

Fig. 1. DSC and TG curves for complex **I**.

dered over two positions. The CPC angles are close to the theoretical value (108.84(11)°–110.90(10)°). The $P–C_R$ distance (1.822(2) Å) is longer than the $P–C_{Ar}$ bonds (1.790(2)–1.796(2) Å). The planes of three phenyl rings are nearly perpendicular to each other in order to minimize intramolecular interactions, and the slopes are as follows: 88.94° between C(1)–C(6) and C(11)–C(16), 87.17° between C(11)–C(16) and C(21)–C(26), and 77.81° between C(1)–C(6) and C(21)–C(26).

The planar square coordination of the platinum atom in the $[PtCl_4]^{2-}$ anion is not distorted. The anion is highly symmetric, i.e., has symmetry planes Cl(1)PtCl(2) and Cl(1')PtCl(2'). The platinum atom is located in the inversion center, and the Pt–Cl bond lengths are 2.304(10) and 2.312(11) Å, which are somewhat shorter than the covalent radii of the platinum and chlorine atoms (2.35 Å) [32] and almost the same as in similar $[PtCl_4]^{2-}$ anions [21, 23]. The ClPtCl *trans*-angles are 180°, and the ClPtCl *cis*-angles are 89.57(3)° and 90.43(3)°. The presence of short contacts between the cations and anions is a specific feature of the structures of tetraorganylphosphonium haloplatinates. Each cation is bound to two anions by weak interionic contacts $C_{Ar}–H\cdots Cl$ (2.77–2.853 Å) and O–H···Cl (2.35–2.87 Å) (Fig. 3). Each cation interacts with two adjacent cations to form chains of the cations. The *meta*-protons of the phenyl ring form weak contacts with the carbon atoms of the phenyl ring ($C–H\cdots C_{Ar}$ 2.82 Å) and oxygen atoms (C–H···O 2.52 Å) of the adjacent cations. The supporting contacts C–O···Cl (3.13 Å) are observed between the cations and anions, composing 95% of the sum of van der Waals radii of the contacting atoms [33]. Each anion is surrounded by four cations to form a chain shielded from both sides with the chains of the cations along the crystallographic acid *c*. No short contacts are observed between the anions because of a large size of phosphonium cations.

Dichlorobis(triphenylphosphine)platinum is known to exist in the *cis*- and *trans*-isomeric forms [34, 35], and the *trans*-isomer is prepared by the photochemical isomerization of the *cis*-$[PtCl_2(PPh_3)_2]$ complex [31].

The structures of the triclinic modification of *trans*-dichlorobis(triphenylphosphine)platinum and of the orthorhombic modification containing two dichloromethane molecules were presented in [31] and [35], respectively.

The crystals of the *trans*-$[PtCl_2(PPh_3)_2]$ complex (**II**·$CHCl_3$) have a monoclinic modification. The platinum atom of complex **II**·$CHCl_3$ has a planar square coordination mode, and the bulky phosphine ligands have *trans*-orientation (Fig. 2b). The bond lengths and bond angles of complex **II**·$CHCl_3$ are close to similar values in *trans*-$[PtCl_2(PPh_3)_2]$ [34] and *trans*-$[PtCl_2(PPh_3)_2]\cdot 2CH_2Cl_2$ [35]. The Pt–P bond lengths are 2.3224(17), 2.3163(11) Å [34] and 2.3095(7) Å [35], and Pt–Cl are 2.3119(18), 2.2997(11) Å [34] and 2.3086(7) Å [35]. The platinum atoms have a distorted planar square geometry: P(1)PtCl(1) 87.47(5)° (87.88(4)° [34], 86.62(3)° [35]) and P(1)PtCl(2) 92.52(5)° (92.12(4)° [34], 93.38(3)° [35]), and the *trans*-angles P(1)PtP(2) and Cl(1)PtCl(2) are equal to 180° ($^{i}\,1-x, 1-y, 2-z$). The obtained values somewhat differ from similar values in *cis*-$[PtCl_2(PPh_3)_2]$ characterized by steric hindrances [31]. The P–C bond lengths vary in a range of 1.796(4)–1.854(4) Å,

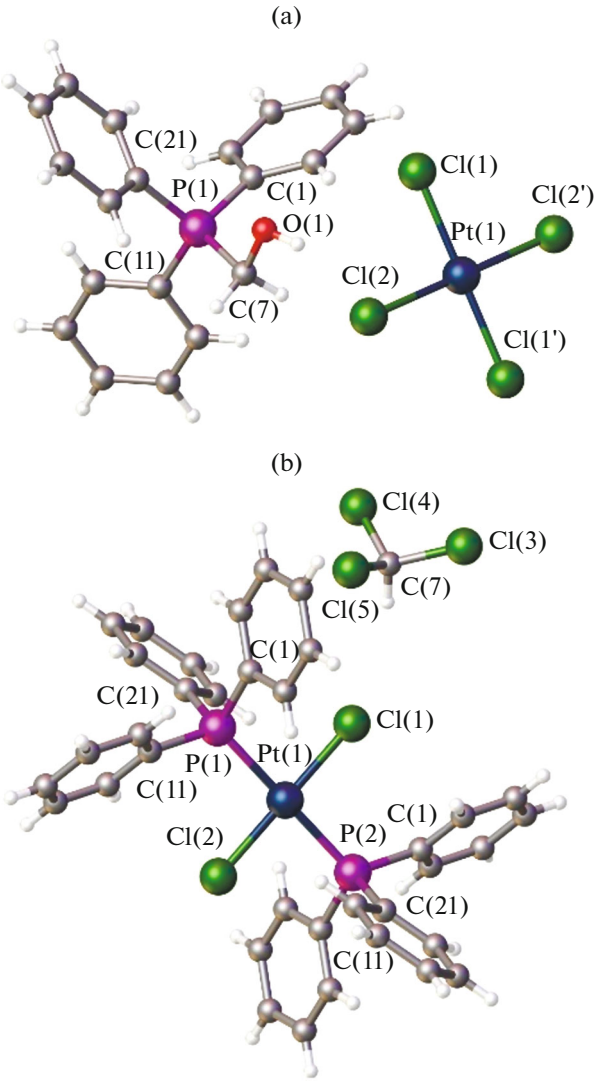

Fig. 2. General view of complexes (a) **I** and (b) **II**·$CHCl_3$.

and the C(1)P(1)Pt angle (118.95(16)°) significantly deviates from two other angles (109.48(15)° and 113.41(17)°). The solvate chloroform molecule is disordered over four positions with a population of 0.25. One phenyl ring is disordered over two positions with contributions of 0.5/0.5, and two other phenyl rings are disordered over two positions with contributions of 0.48/0.52.

The crystal structure of complex **II**·$CHCl_3$ is stabilized by intermolecular contacts C–H···H (2.1 Å) and C–H···C (2.3, 2.8 Å) (Fig. 4). The spatial network of the crystal is formed due to hydrogen bonds involving the hydrogen atom of the solvate chloroform molecule and chlorine atom of the molecular complex C–H(7)···Cl(2) (2.9 Å).

Thus, the reaction of hexachloroplatinic acid with (hydroxymethyl)triphenylphosphonium chloride in an acetonitrile–water mixture is accompanied by the reduction of platinum(IV) to platinum(II). The formation of a mixture of the platinum(II) complexes $[Ph_3PCH_2OH]_2[PtCl_4]$ and *trans*-$[PtCl_2(PPh_3)_2]$ is caused by the transformation of the cation accompanied by the elimination of formaldehyde that acts as a reducing agent. Specific features of the structures of the synthesized complexes were studied by XRD.

The complex of (hydroxymethyl)triphenylphosphonium tetrachloroplatinate(II) (**I**) was shown to be unstable on dissolving in diethyl sulfoxide or on heating and transforms into the molecular complex of *trans*-dichlorobis(triphenylphosphine)platinum (**II**).

These reactions represent new and easy methods for the synthesis of *trans*-dichlorobis(triphenylphosphine)platinum, which is used as an intermediate

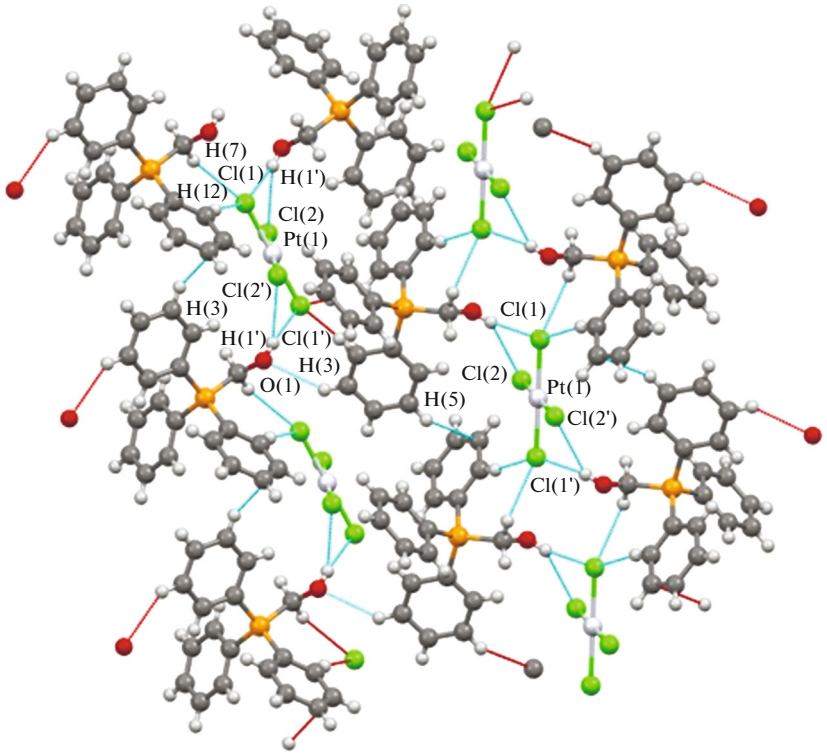

Fig. 3. Packing of cations and anions in the crystal of complex **I**.

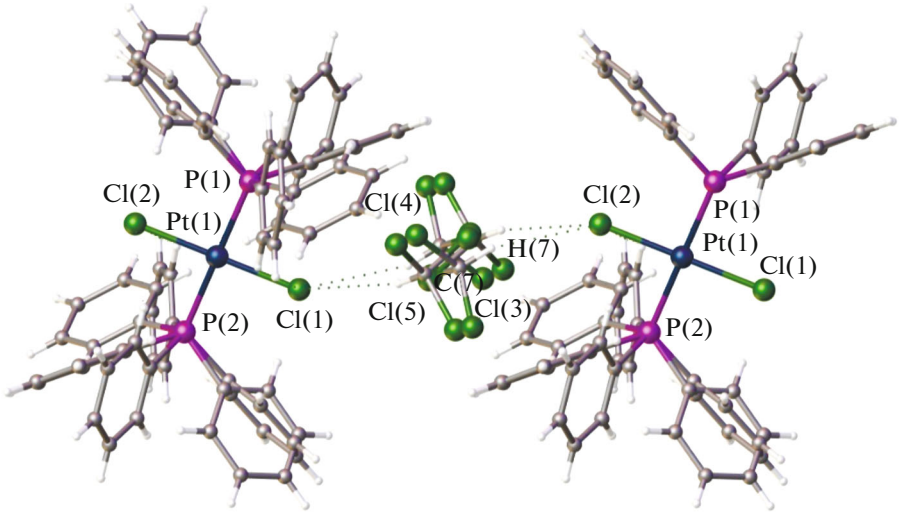

Fig. 4. Intermolecular interactions in complex **II**·$CHCl_3$.

compound in the synthesis of other platinum complexes.

ACKNOWLEDGMENTS

The authors are grateful to D.A. Zherebtsov for performing differential scanning calorimetry.

CONFLICT OF INTEREST

The authors declare that they have no conflicts of interest.

REFERENCES

1. Kulinchik, T., V, *Meditsinskie Tekhnologii, Otsenka i Vybor*, 2013, vol. 1, p. 87.

2. Hizal, S., Hejl, M., Jakupec, M.A., et al., *Inorg. Chim. Acta*, 2019, vol. 491, p. 76.
3. Varbanov, H.P., Jakupec, M.A., Roller, A., et al., *J. Med. Chem.*, 2013, vol. 56, p. 330.
4. Gramatica, P., Papa, E., Luini, M., et al., *J. Biol. Inorg. Chem.*, 2010, vol. 15, p. 1157.
5. Galanski, M., Jakupec, M.A., and Keppler, B.K., *Curr. Med. Chem.*, 2005, vol. 12, p. 2075.
6. Johnstone, T.C., Suntharalingam, K., and Lippard, S.J., *Chem. Rev.*, 2016, vol. 116, no. 5, p. 3436.
7. ÖğütçüH., Yetim, N.K., and Ozkan, E.H., *Pol. J. Chem. Tech.*, 2017, vol. 19, no. h. 2017, p. 74.
8. Watanabe, T., Takano, M., Ogasawara, A., et al., *Antimicrob. Agents. Chemother.*, 2000, vol. 44, p. 2853.
9. Ura, Y., Gao, G., Bao, F., et al., *Organometallics*, 2004, vol. 23, p. 4804.
10. Lukin, R.Yu., Kuchkaev, A.M., Sukhov, A.V., et al., *Polymers*, 2020, vol. 12, no. 10, p. 2174.
11. Meister, T.K., Riener, K., Gigler, P., et al., *ACS Catal.*, 2016, vol. 6, p. 1274.
12. Troegel, D. and Stohrer, J., *Coord. Chem. Rev.*, 2011, vol. 255, p. 1440.
13. Cotton, F.A. and Francis, R., *J. Am. Chem. Soc.*, 1960, vol. 82, p. 2986.
14. Meek, D.W., Straub, D.K., and Drago, R.S., *J. Am. Chem. Soc.*, 1960, vol. 82, p. 6013.
15. Bokach, N.A., Izotova, Yu.A., and Haukka, M., *Acta Crystallogr., Sect. E: Struct. Rep. Online*, 2007, vol. 63, p. 1261.
16. Popa, A., Davidescu, C., Trif, R., et al., *React. Funct. Polym.*, 2003, vol. 55, p. 151.
17. Masayo, I., Tomoo, I., and Biyuuki, K., Jpn. Patent, 2002, p. 2002308713.
18. Satoshi, H. and Hideto, O., Jpn Patent, No. 2000263706, 2000.
19. Galkina, I.V. and Egorova, S., *Medical Almanac. Pharm.*, 2009, vol. 8, p. 142.
20. *Cambridge Crystallographic Database*, Cambridge, Release 2021.
21. Kuzniak-Glanowska, E., Glosz, D., Niedzielski, G., et al., *Dalton Trans.*, 2021, vol. 50, p. 170.
22. Albrecht, C., Steinborn, D., and Lis, T., *CSD Communications*, 2019, p. 1895372.
23. Suslonov, V.V., Eliseeva, A.A., Novikov, A.S., et al., *CrystEngComm*, 2020, vol. 22, no. 24, p. 4180.
24. Rheingold, A.L., *CSD Communications*, 2017, p. 1573034.
25. Tkacheva, A.R., Sharutin, V.V., Sharutina, O.K., et al., *J. Gen. Chem.*, 2019, vol. 89, p. 1816.
26. Chernyaev, I.I., *Sintez kompleksnykh soedinenii metallov platinovoi gruppy* (Synthesis of Complex Compounds of Platinum Group Metals) Moscow: Nauka, 1964.
27. *SMART and SAINT-Plus. Versions 5.0*, Madison: Bruker AXS Inc., 1998.
28. *SHELXTL/PC. Versions 5.10. An Integrated System for Solving, Refining and Displaying Crystal Structures from Diffraction Data*, Madison: Bruker AXS Inc., 1998.
29. Dolomanov, O.V., Bourhis, L.J., and Gildea, R.J., et al., *J. Appl. Crystallogr.*, 2009, vol. 42, p. 339.
30. Huang, W. and Xu, J., *Synth. Commun.*, 2015, vol. 45, p. 1777.
31. Johansson, M.H. and Otto, S., *Acta Crystallogr., Sect. C: Struct. Sci.*, 2000, vol. 56, p. 12.
32. Cordero, B., Gomez, V., Platero-Prats, A.E., et al., *Dalton Trans.*, 2008, vol. 21, p. 2832.
33. Mantina, M., Chamberlin, A.C., Valero, R., et al., *J. Phys. Chem. A*, 2009, vol. 113, p. 5806.
34. Fun, H.K., Chantrapromma, S., Liu, Y.C., et al., *Acta Crystallogr., Sect. E: Struct. Rep. Online*, 2006, vol. 62, p. 1252.
35. Sunkel, K., Bernhartzeder, S., and Birk, U., *Z. Naturforsch*, 2012, vol. 67, p. 557.

Translated by E. Yablonskaya